N91-14982

TEMPERATURE DISTRIBUTION OF DUST IN LUMINOUS IRAS GALAXIES

David P. Carico
Downs Laboratory of Physics, 320-47
California Institute of Technology, Pasadena, CA 91125

INTRODUCTION

Work is currently in progress to obtain temperature distributions of dust in the most infrared-luminous galaxies. The results presented herein are of a preliminary nature, representing a zeroth-order approximation (see **WORK YET TO BE DONE**, below). The objects which have been analyzed so far are all galaxies from the *IRAS* Bright Galaxy Sample with infrared luminosities $L_{IR} \geq 10^{11}\ L_{\odot}$ (see Carico *et al.*, 1988). They are: **Arp 220, Mrk 231, Mrk 273, NGC 1614, NGC 3690, NGC 6285/6,** and **Zw 049.057**. The analysis utilized 3.7 μm data from the Palomar 5 m Hale telescope, *IRAS* data at 12, 25, 60, and 100 μm, and 1 mm continuum data from the CalTech Submillimeter Observatory on Mauna Kea.

METHOD

A cloud of N spherical dust grains at a distance d from the observer produces an observed flux density at a wavelength λ given by

$$f_\nu(\lambda) = \int_0^\infty \pi B_\nu(\lambda, T) \left(\frac{a}{d}\right)^2 Q_{abs}(\lambda) \frac{dN}{dT} dT \,, \tag{1}$$

where a is the radius of the dust grains, $Q_{abs}(\lambda)$ is the absorption efficiency of the dust grain material, and $B_\nu(\lambda, T)$ is the Planck function. If a mean mass density is adopted for the grain material (a value of 3 g cm^{-3} was used to obtain the accompanying results), N can be rewritten in terms of the total mass of dust, M, and eqn. (1) can be put in the form

$$f_\nu(\lambda) = C\, \frac{Q_{abs}(\lambda)}{a} \frac{1}{\lambda^3} \int_0^\infty \frac{1}{e^{\frac{hc}{\lambda kT}} - 1} \frac{dM}{dT} dT \,, \tag{2}$$

where C is a constant for a given emission source, depending only on the mean mass density of the grain material and the distance to the source. For $\lambda \gg a$, the quantity $Q_{abs}(\lambda)/a$ is independent of a (see, e.g., Hildebrand, 1983); thus, for infrared emission from spherical interstellar dust grains, the observed flux density does not depend on the size of the grains.

In numerical form, eqn. (2) becomes

$$f_\nu(\lambda_i) = C\, \frac{Q_{abs}(\lambda_i)}{a} \frac{1}{\lambda_i^3} \sum_j \frac{1}{e^{\frac{hc}{\lambda_i kT_j}} - 1} \left(\frac{dM}{dT}\right)_j dT_j \,.$$

Using logarithmic intervals for λ and T, so that $\lambda_i = \lambda_o\, x^i$, $T_j = T_o\, y^j$, and $dT_j = T_j - T_{j-1} = T_j(1 - \frac{1}{y})$, where x, y, λ_o, and T_o are constants, and defining

$$f_i = \frac{\lambda_o^3 a}{C Q_{abs}(\lambda_i)} (1 - \frac{1}{y})\, f_\nu(\lambda_i)$$

$$K_{ij} = \left[x^i (e^{\frac{hc}{\lambda_i kT_j}} - 1)\right]^{-1}$$

$$g_j = \left(\frac{dM}{d(\ln T)}\right)_j$$

PAGE 324 INTENTIONALLY BLANK

PRECEDING PAGE BLANK NOT FILMED

one obtains

$$f_i = \sum_j K_{ij} \, g_j \tag{3}$$

which must be solved for the g_j.

For the analysis presented here, eqn. (3) was solved using a modified version of the least-squares computer program described by Pajot *et al.* (1986) (which was generously provided by J. L. Puget when this author's own program failed to cooperate for as yet unknown reasons – my sincerest thanks!). A wavelength range from 3.7 μm to 1000 μm was used for all objects. The results are shown in the accompanying figures.

RESULTS

The results for three representative galaxies are shown in Figures 1 and 2. In each plot, three curves have been drawn, representing results for three different emissivity laws:

$$Q_{abs} \propto \lambda^{-1}\text{: solid line}$$
$$Q_{abs} \propto \lambda^{-1.5}\text{: dotted line}$$
$$Q_{abs} \propto \lambda^{-2}\text{: dot – dashed line}$$

where Q_{abs} is the absorption efficiency, normalized to $Q_{abs}(100\ \mu m)/a = 133.3\ \mathrm{cm}^{-1}$, and a is the effective grain size.

Figure 1 shows the mass of dust (in units of $M_\odot = 2 \times 10^{33}$ gm) per logarithmic temperature interval. The total mass is thus the area under the curve shown.

In Figure 2 is shown the fraction of the total luminosity emitted by dust at a temperature T (in the top half of each plot), and the fraction of the luminosity which is being emitted by dust which is at temperatures $\geq T$. These plots tend to bring out the differences between the galaxies much more clearly than the mass distribution plots of Figure 1, due to the extreme temperature dependence of the luminosity ($L \propto T^{4+\beta}$, for $Q_{abs} \propto \lambda^{-\beta}$). In particular, one can compare the very sharply peaked distribution for Arp 220, centered at 50 K, and falling to 5% of the luminosity at temperatures $\lesssim$ 25 K and $\gtrsim$ 100 K, with the broad distribution for Mrk 231, which peaks at roughly 150 K and falls to 5% of the luminosity for temperatures $\lesssim$ 40 K and $\gtrsim$ 350 K. This difference can also be seen in the bottom plots where, for Arp 220, $\lesssim$ 10% of the luminosity is being emitted by dust with temperatures $>$ 100 K, whereas for Mrk 231, the contribution to the luminosity from $T >$ 100 K dust is $\sim$ 60%.

Figure 2 also indicates how uncertain estimates of the mass of cold dust can be. For the case of Mrk 231, Figure 2 suggests that more than 90% of the luminosity is being emitted by dust at temperatures $\gtrsim$ 50 K. However, from Figure 1 it is seen that most of the estimated dust mass for Mrk 231 is at temperatures $\lesssim$ 50 K. Hence, significant changes in the total mass of dust would not necessarily be reflected in the energy distribution.

WORK YET TO BE DONE

As mentioned previously, the work presented here is preliminary, intended to obtain a qualitative feel for the analysis and the results that can be obtained. The main simplifications which have gone into this analysis, and which will be addressed in subsequent work, are as follows:

1. The dust was assumed to be everywhere optically thin to infrared radiation. This is almost certainly not the case, particularly for the compact central regions of such galaxies as Arp 220 and Mrk 231.
2. The 1 – 3 μm data has not yet been utilized, due to the complexities of accurately accounting for contamination from stellar emission. These wavelengths will clearly be important in understanding the hottest dust, particularly for temperatures in excess of 1000 K.
3. The contribution to the emission from very small grains, presumably PAHs (polycyclic aromatic hydrocarbons), has not been addressed, and may be significant in some sources.

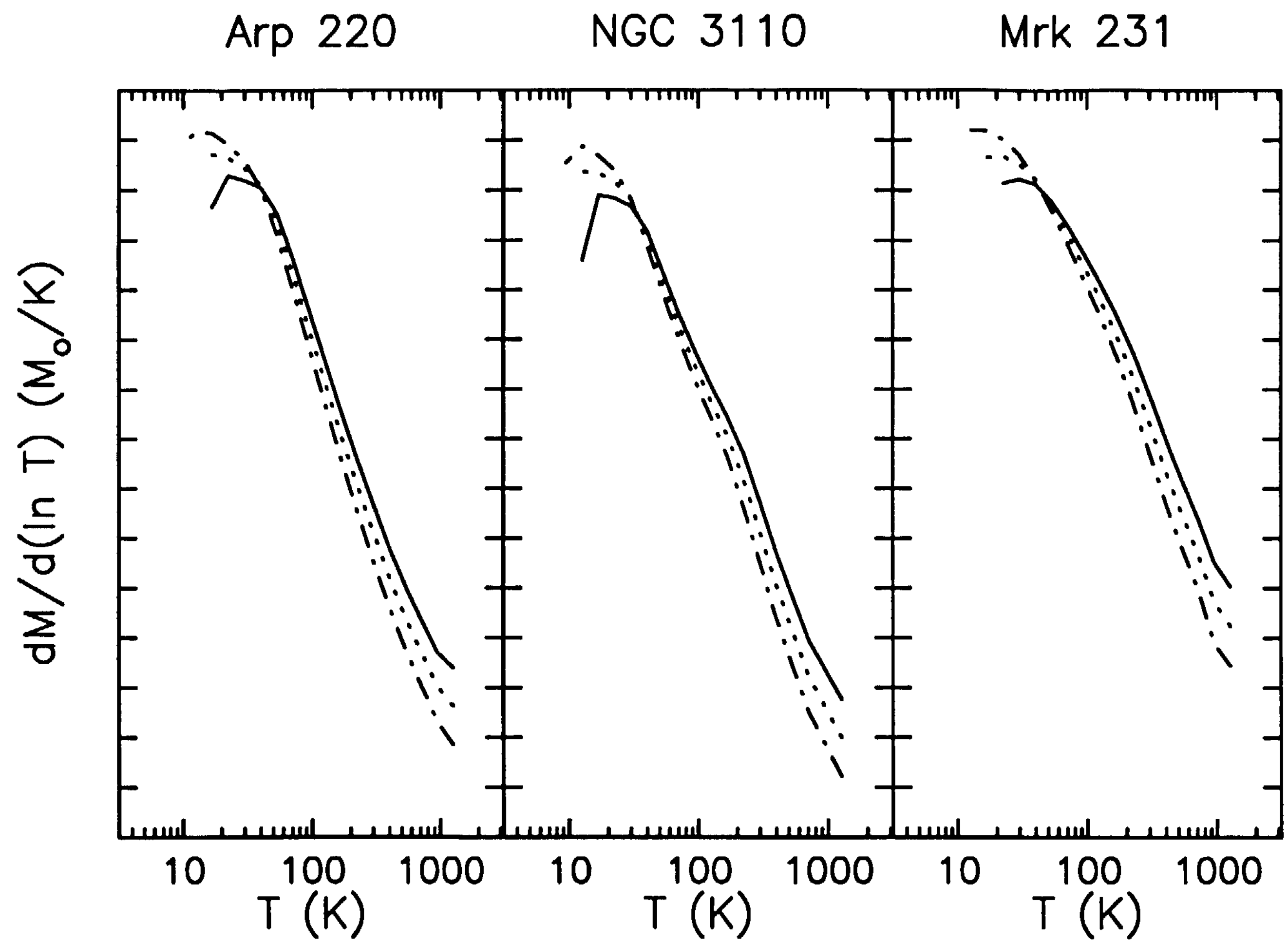

Figure 1: The mass of interstellar dust as a function of temperature for three infrared-luminous galaxies. The different curves on each plot are discussed in the text.

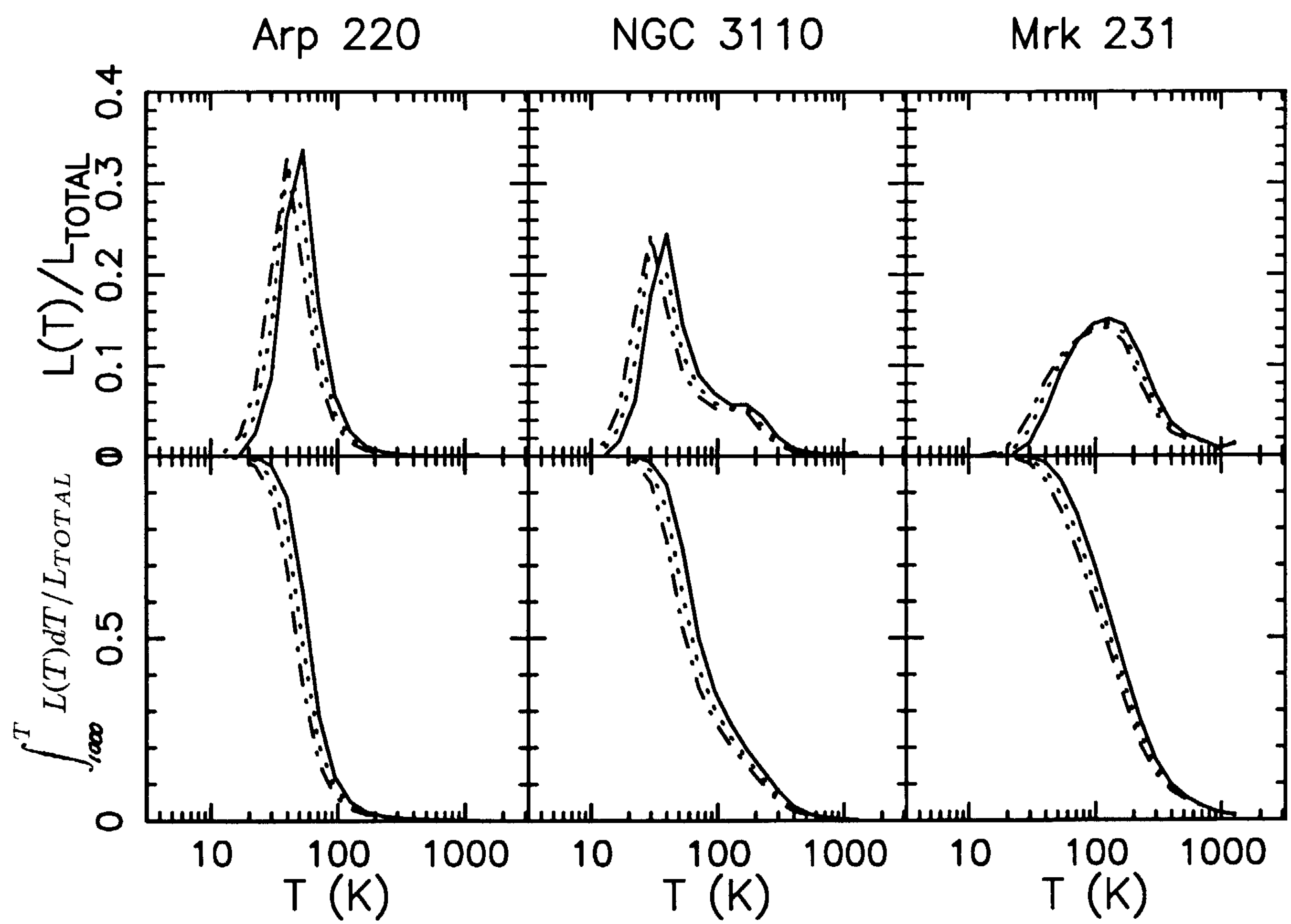

Figure 2: (*top*) The fraction of the luminosity emitted by dust at temperature T (*bottom*) The fraction of the luminosity emitted by dust at all temperatures $\geq T$.

The author is grateful to J. L. Puget and B. T. Soifer for extremely helpful discussions, J. Keene for vital assistance in obtaining the 1 mm measurements at the CalTech Submillimeter Observatory, and B. T. Soifer and G. Neugebauer for financial support while attending the symposium.

REFERENCES

Carico, D.P., Sanders, D.B., Soifer, B.T., Elias, J.H., Matthews, K., and Neugebauer, G.: 1988, *Astron.J*, **95**, 356.

Hildebrand, R.H.: 1983, *Q.J.R.A.S.*, **24**, 267.

Pajot, F., Boissé, P., Gispert, R., Lamarre, J.M., Puget, J.L., and Serra, G.: 1986, *Astron.Astrophys.*, **157**, 393.